(CCSBT-ERS/2406/BGD 01
(Previously CCSBT-ERS/2203/12-A and B)
(ERSWG Agenda item 5.1.2)

Fisheries New Zealand
Tini a Tangaroa

Assessing inter-annual variability in Antipodean albatross distribution

New Zealand Aquatic Environment and Biodiversity Report xx

Y. Richard,
L. Tremblay-Boyer,
K. Berkenbusch,
N. Wilkinson,
K. Walker,
G. Elliott

ISSN 1179-6480 (online)
ISBN xxx-x-xx-xxxxxx-x (online)

April 2024

Te Kāwanatanga o Aotearoa
New Zealand Government

Disclaimer

Requests for further copies should be directed to:

Fisheries Science Editor
Fisheries New Zealand
Ministry for Primary Industries
PO Box 2526
Wellington 6140
NEW ZEALAND

Email: Fisheries-Science.Editor@mpi.govt.nz
Telephone: 0800 00 83 33

This publication is also available on the Ministry for Primary Industries websites at:
http://www.mpi.govt.nz/news-and-resources/publications
http://fs.fish.govt.nz go to Document library/Research reports

Please cite this report as:

Richard, Y.; Tremblay-Boyer, L.; Berkenbusch, K.; Wilkinson, N.; Walker, K.; Elliott, G. (2024). Assessing inter-annual variability in Antipodean albatross distribution. *New Zealand Aquatic Environment and Biodiversity Report xx*. 24 p.

TABLE OF CONTENTS

EXECUTIVE SUMMARY

Y. Richard*; L. Tremblay-Boyer†; K. Berkenbusch*; N. Wilkinson*; K. Walker‡; G. Elliott†
(2024). Assessing inter-annual variability in Antipodean albatross distribution.

***New Zealand Aquatic Environment and Biodiversity Report No. XXX*. 24 p.**

This study assessed the temporal variability in seabird distributions estimated from tracking data and its impact on a key derived output, the spatial overlap with fisheries. It used Antipodean albatross (sub-species *Diomedea antipodensis antipodensis*) as a case study, owing to the availability of long-term tracking data for this sub-species, and a recent increase in tracking effort across life stages.

The analysis confirmed key spatial differences in the distribution of Antipodean albatross by breeding status, age, and sex. Considering these differences led to an improved distribution map of all life stages combined, which integrated all available tracking data with weights by life stage from a recently-updated population model. The distribution map was compared with surface-longline fishing effort in the Southern Hemisphere to assess variability in particular areas of overlap with fisheries ("overlap hotspots"); this temporal assessment included the application of an overlap statistic. Although there was variability in the location of overlap hotspots through time, there were distinct areas that were consistently classified as overlap hotspots in the time period from 1997 to 2019. These areas included the Tasman Sea, an area eastward and northward of New Zealand's North Island, and off the coast of Chile.

The development of the distribution maps included the testing of a resampling-based approach to assess the differences in distribution overlap across time periods via randomisation. This testing found that other track features, such as the track length (measured in the number of observations) also needed to be accounted for when comparing distributions across time periods. This aspect is particularly relevant to seabird species for which multiple tag types have been used throughout the time series of tracking data. In the current analysis, there was some support for a change in distribution for non-breeding females over time. Nevertheless, the differences was not significant, possibly owing to the small number of tracks in early years.

The approach used here, of applying the overlap statistic to assess overlap hotspots and their consistency through time, is broadly applicable to other seabird species with tracking data.

The findings from this research were presented at the 14th meeting of the Ecologically Related Species Working Group (ERSWG14) of the Commission for the Conservation of Southern Bluefin Tuna in March 2022. Since then, discrepancies in the tracking data have been corrected, leading to updated distribution maps of Antipodean albatross.

* Dragonfly Data Science, New Zealand † CSIRO, Australia ‡ Albatross Research, New Zealand

1. INTRODUCTION

Species distributions for seabirds can be difficult to quantify because individuals have an extensive range but may use specific areas intensively (e.g., Waugh et al. 2002). In addition, area use can change over time and across breeding status (e.g., Rayner et al. 2012, Pettex et al. 2017a, Pettex et al. 2017b). At the same time, knowledge of the spatial distribution of seabirds is important for assessing threats to their populations, such as bycatch mortality in fisheries (Grémillet et al. 2018, Calado et al. 2021). Determining the spatial and temporal overlap of seabird distributions with fisheries allows the identification of particular areas with high numbers of fishery interactions (e.g., Ramos et al. 2017).

In the Southern Hemisphere, previous research into the risk of surface-longline fisheries to albatrosses and petrels focused on 26 taxa that breed in the Southern Hemisphere (including the two sub-species of Antipodean albatross, *Diomedea antipodensis antipodensis* and *D. a. gibsoni*) and are listed under the Agreement of the Conservation of Albatrosses and Petrels (Abraham et al. 2017, Abraham et al. 2019). The previous assessments developed distribution maps for key life stages of the 26 taxa from tracking data, following a methodology similar to that described by Carneiro et al. (2020). Seabird distributions are particularly important in the application of spatial risk assessment that combine seabird distributions and fishing effort data to generate predictions of particular areas of high capture. The identification of these areas has been proposed as a tool for the spatial management of the surface-longline fishery in the Commission for the Conservation of Southern Bluefin Tuna (CCSBT) convention area.

The previous analysis by Abraham et al. (2019) highlighted three limitations for the development of seabird distributions from tracking data: first, tracking data were not available for all species, life stages, and sites, so that distribution data needed to be augmented with existing range maps that lacked density information; second, the generated distributions were static, i.e., all available tracking data were combined into a single distribution applied to all years; if seabird distributions vary between years, any management relying on the average location of high-use areas ("distribution hotspots") across years might not be effective; third, distributions derived from observations only are dependent on the behaviour of individual birds, and high-use areas might be excluded by chance if none of the tracked individuals use them during tracking. This latter aspect is of particular concern for species for which little tracking data are available.

In the previous analyses, a key challenge for attempting to address these limitations was the availability of tracking data for most seabird species. Nevertheless, since then, there have been 158 000 new locations recorded for the Antipodean albatross sub-species *D. a. antipodensis*. In addition, previous research has identified potential changes in the distribution of this species for some life stages (Carneiro et al. 2020). Based on the data-rich tracking dataset, Antipodean albatross was used here as a case study to explore some of the limitations raised in the previous analysis by Abraham et al. (2019).

In the present study, the temporal variability in distributions was re-assessed in view of the availability of increased tracking data throughout the time series. This re-assessment included the development of an approach to test for changes in distribution between time periods. It also included the application of a hotspot metric across life stages and over time to assess variability in high-use areas. In addition, a life-stage weighted distribution for all individuals was generated and compared with surface-longline fishing effort data from the Southern Hemisphere.

2. METHODS

2.1 Input tracking data and data preparation

Satellite tags and global location sensing (GLS) loggers for Antipodean albatross were deployed from 1996 onwards (by two of the authors, K. Walker and G. Elliott, who also processed the data from the GLS loggers). The data is curated by New Zealand's Department of Conservation. The 2019 risk assessment (Abraham et al. 2019) used an externally-prepared version of this dataset (from the Birdlife International

Seabird Tracking Database); however, because recent years of tagging data for Antipodean albatross were missing from this dataset, the data preparation here was repeated for internal consistency, based on the original tracking data for the period from 1996 to 2022.

Tracking data were collected using tracks from satellite and GLS tracking devices for the period from 1997 to 2021. Geographical coordinates were directly available for satellite tags. For GLS tags, locations were estimated from the sunlight measurements and sea surface temperature recorded by the tracking device. The probGLS algorithm (Merkel et al. 2016) was used to generate a most-likely track from the median of the predicted locations for each observation. This approach estimates location with an error of less than 200 km (Merkel et al. 2016), but precision changes throughout the year, and is lower close to the equinoxes. Once a most-likely track was estimated for GLS tags, all locations for satellite and GLS tags were collated into a single dataset.

Life-history covariates were also available from the field data (collected by two of the authors, G. Elliott and K. Walker),including the breeding status, sex, and age of tagged individuals. Based on this information, individuals were categorised as "breeding adults", "non-breeding adult or pre-breeder", or "juvenile".

Records of individual bird locations were prepared using the following set of rules:

- records were removed if locations or dates were outside of latitudes 90 °S to 90 °N and time period 1997 to 2021;
- records from satellite tags were removed when their quality was labelled as "Z" (i.e., invalid);
- GLS records were removed if they were within 30 days of the equinox due to their unreliable locations;
- records were removed if the speed of an individual from a previous location or to the next location (in km/h, based on great circle distances) was in excess of 100 km/h;
- records from satellite tags and GLS were removed if they were within 10 km and 100 km from the colony, respectively, to exclude birds at the colony while taking into account the inaccuracy in the locations;
- locations on land were excluded.

The tracks were then split into separate segments when there were gaps longer than 24 hours between successive locations, and segments consisting of a unique location were discarded. The prepared location records were interpolated at regular time intervals of 30 minutes within each segment, assuming linear displacement between records. No locations were interpolated between separate segments. The interpolated records were assumed to reflect occupancy over the spatial range of the study.

Following Abraham et al. (2019) and Carneiro et al. (2020), the gridded distributions were then generated by summing over all the interpolated records in each pixel of a pre-defined distribution 1-degree-resolution grid, for each sex and breeding status. Each density was finally standardised so that all cells weighted by their area summed to 1, and the standardised densities were multiplied by the number of individuals in each class of the population (by sex and breeding status), resulting in densities expressed in birds.km^{-2}.

The number of individuals in each class was obtained from a Bayesian integrated population model of the species, updated from Richard (2021) (Table 1). The population model was fitted to capture-recapture data collected every year since 1994 within a subset of the whole colony at Antipodes Island. The population structure was simulated over the study period, modelling the fate of each individual using the state transitions estimated in the model; the structure of the simulated population in 2021 was used

to provide the number of individuals in each stratum. The studied population was then scaled up to the entire population based on the studied population representing 2.73% of the total population, following population surveys of the entire island between 1994 and 1996.

Table 1: Number of individuals in each population class (i.e., sex and breeding status) used to weigh the stratum-level at-sea distributions, obtained from an integrated population model of Antipodean albatross (see Richard 2021).

Status	Gender	No. of individuals
Juvenile	Female	2 591
	Male	2 501
Non-breeding adult or pre-breeder	Female	6 426
	Male	12 076
Unsuccessful breeder	Female	1 408
	Male	1 616
Successful breeder	Female	2 845
	Male	3 276

Each distribution layer was smoothed for cells with less than five birds or that were on the edge by taking a weighted average of the eight neighbouring cells, using weights of 1.0, 0.5, and 0.25, for the focal cell, the cells immediately adjacent, and the diagonal cells, respectively.

To derive the distribution for the entire sub-species, the densities of all population classes were summed.

2.2 Comparing distributions between time periods

An approach to test for differences between the distribution of individuals across different time periods was developed, and tested on male and female non-breeders for the time periods pre-2004 and post-2011. This period was chosen because differences in distributions between the time periods pre-2004 and 2011–2017 were previously noted for these two groups (Elliott & Walker 2017). The periods also represented changes in tagging methods, particularly in the type of tag used (satellite or GLS tags) and overall tagging numbers. As such, the approach also allowed testing of whether changes in tagging methodology can influence the distribution generated from tagging data.

The approach used both resampling and randomisation to test for differences in time periods while accounting for differences in sample size across time periods and differences in track lengths. The reference period included years 1996 to 2004 (pre-2004), and the test period was defined to be the years from 2011 to 2022 (noting no new tags were released from 2005 to 2010). The prepared tracking dataset was filtered to include only non-breeding adults and pre-breeders. The dataset was then split by sex and time period, and a test of differences in distribution was conducted separately for males and females.

For each sex, a kernel density was estimated from tracks selected from the reference and test time periods, using the kernelUD function from the adehabitatHR package (Calenge 2006). All tracks were selected from the reference dataset, given the limited sample size, and a matching number of tracks was randomly selected from the test dataset. There were nine tracks available for the pre-2004 period for non-breeding females, and eleven tracks available for the pre-2004 period for non-breeding males. The overlap between the 95% kernel outlines for the two periods was then measured using the Bhattacharyya's affinity (BA), a metric of spatial overlap between distributions which ranges from 0 (no overlap) to 1 (full overlap) (Fieberg & Kochanny 2005). This measurement was repeated 500 times.

To provide a probabilistic framework to test for a difference in distributions between time periods, the above procedure was repeated with time periods that were randomly assigned to individual birds before the kernel density was built (retaining the same number of tracks for each time period). The values of the

resulting BA were then compared, pair-wise, with the corresponding values from the non-randomised BA to compute the proportion of times the non-randomised BA was smaller than the randomised BA. If there was no difference in distributions through time, the distributions of BA for the non-randomised and the randomised versions of the test are expected to be similar. If there is a difference in distributions through times (indicated by smaller values of BA, because the metric approaches 0 as overlap decreases), the non-randomised BA is expected to be smaller than the randomised version.

A modification to the above procedure was applied separately to test for the influence of changing track lengths through time. Here, the resampled test dataset was further modified to match the track lengths in the reference datasets. Track lengths (in number of records) for the reference birds were randomly re-assigned to the individual birds in the test dataset. Track length for these birds was then shortened to match the reassigned track length, starting from the first record. When the re-assigned track length was longer than the number of records available for a test bird, all records for this test bird were retained. The testing procedure was otherwise repeated to generate non-randomised and randomised distributions of the BA metric.

2.3 Identifying distribution hotspots

Distribution hotspots were quantified for the entire tracking dataset and for subsets by breeding status and/or year. The Getis-Ord G_i^* statistic was used as it both detects hotspots and provides a statistical framework to test for their significance (Getis & Ord 2010; see also Sussman et al. 2019 for a review of hotspot metrics). The G_i^* statistic searches for spatial clusters of data points for each grid cell in comparison to its neighbours. The resulting z-score can be assessed for significance, with higher values more likely to be statistically significant.

Neighbour cells were defined as cells that share a border with the focal cell (i.e., each cell has four neighbours, except for cells at the edge of the grid), using the function poly2nb in the R package spdep. The G_i^* statistic was computed using the function localG (also from the R package spdep).

The G_i^* value was calculated for each cell and year, and distribution hotspots were identified by selecting the cells with a z-score above 2.575829, corresponding to a confidence level of 99%. The inter-annual stability of distribution hotspots was calculated as the proportion of years when the cell was selected as a hotspot.

2.4 Overlap between Antipodean albatross and surface-longline fisheries

To assess variability in overlap hotspots between Antipodean albatross and surface-longline fishing effort, the at-sea distribution of the whole species at the 1-degree scale was used. This distribution combined the tracking data from all years, and could not be produced for separate years owing to the lack of tracking data for most demographic strata (i.e., gender and breeding status).

A dataset of surface-longline fishing effort was collated by the National Institute of Water and Atmospheric Research (NIWA) from data provided by regional fisheries management organisations (RFMOs), gridded at a resolution of 5 degrees by 5 degrees. This dataset was considered to include all surface-longline fishing effort in the Southern Hemisphere. The data were provided for the period from 1952 to 2019, but were filtered to only include years from 1997 to 2019, to match the period covered by the available tracking data. In the study area, most of the fishing effort was from the Western & Central Pacific Fisheries Commission (WCPFC), and also from the Inter-American Tropical Tuna Commission (IATTC), the Commission for the Conservation of Southern Bluefin Tuna (CCSBT), the International Commission for the Conservation of Atlantic Tunas (ICCAT), and the Indian Ocean Tuna Commission (IOTC).

This dataset of fishing effort had a number of limitations, including omission of some national fishing effort within Exclusive Economic Zones, incomplete data provision from some RFMO members, and

incomplete data on effort or vessel flag (Francis & Hoyle 2019).

The grid of fishing effort was first converted to a resolution of 1-degree by 1-degree to match the resolution of the bird distribution, after multiplying the effort density from each 5-degree cell by the area of each 1-degree cell (i.e., assuming that effort was distributed evenly across each 5-degree cell). The resolution was increased to 1 degree to retain a maximum amount of information from the Antipodean albatross distribution.

Overlap between surface-longline fisheries and Antipodean albatross was calculated by multiplying the fishing effort (in hooks) and the bird density (in birds.km^{-2}) in each grid cell.

The overlap and the hotspot statistic G_i* were calculated for each year of fishing. Hotspot consistency across years was assessed by counting the number of times each cell was assigned to a hotspot with 99% confidence.

3. RESULTS

3.1 Characterisation of the input dataset

Following the data preparation, tracking data were available for Antipodean albatross for tags deployed between 1996 and 2001, 2003 and 2004, and 2011 to 2022 (Figure 1). The number of tags with data available each year was below 20 for all years up to 2019; subsequently, the number of tags increased to over 60 tags each in 2019 and 2020, 46 tags in 2021, and 41 tags in 2022. There were some changes in the tagging devices deployed over time: satellite devices were deployed exclusively up to 2004, then GLS devices between 2011 and 2018; mostly satellite devices were used after 2019.

Tag data for both males and females were available for each year of the time series, with a slightly higher proportion of females (Figure 1). Tags were deployed almost exclusively on adults up to 2019, after which more than a third of deployed tags was on juveniles in 2019, 2020, and 2022. The distribution of breeding status changed over time, with a higher proportion of breeders in earlier tagging years.

Track length, measured in days with at least one recorded position, varied over time; most tag data from the earlier time period were shorter than six months (Figure 2). For data from tags between 2011 and 2018, when all tags were of type GLS, the tracks often exceeded one year in length (with some tracks spanning up to two years).

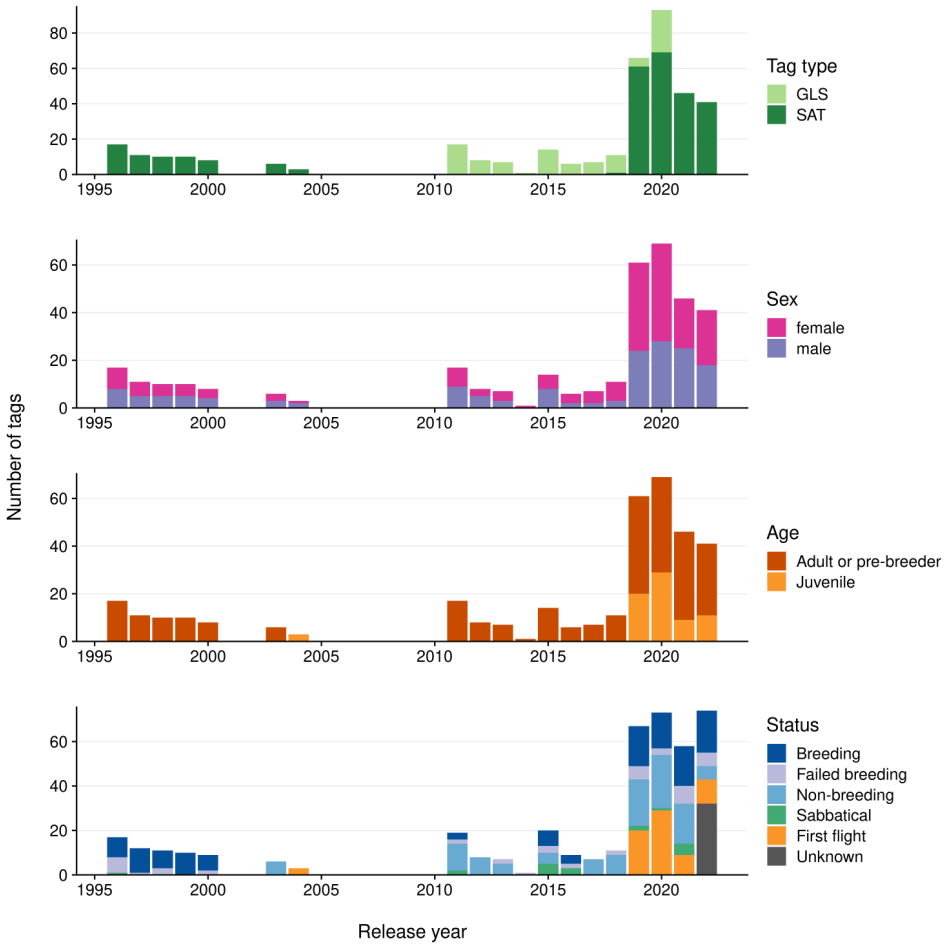

Figure 1: Overview of prepared tracking dataset for Antipodean albatross by type of tagging device, individual sex, age, and breeding status. Tracking data were collected with global location sensing (GLS) and satellite (SAT) tracking devices.

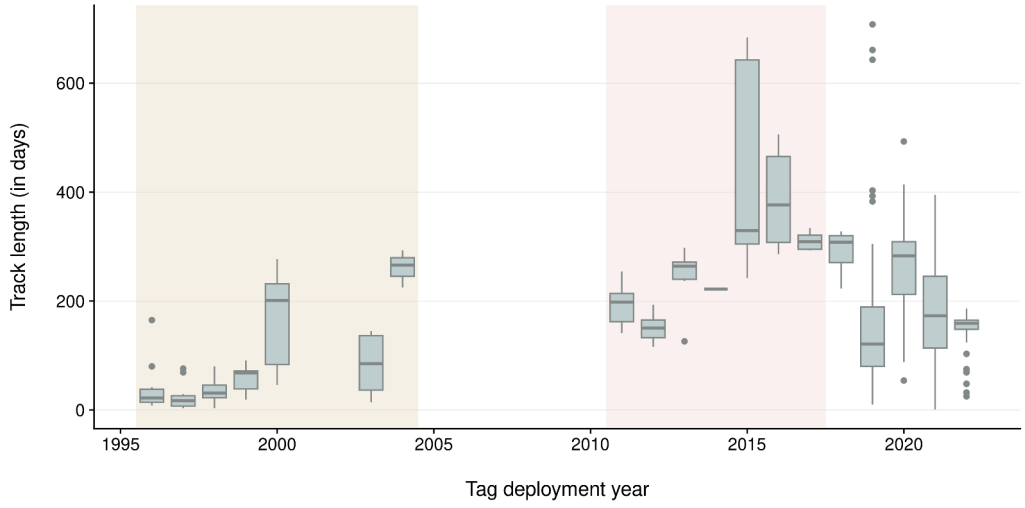

Figure 2: Distribution of track length (in number of days) by individual Antipodean albatross tagged, shown by release year. Boxplot shows the interquartile range, with the median as bold horizontal line; light yellow and pink boxes highlight periods when all tags were satellite tags and global location sensing (GLS) tags, respectively.

3.2 Trends in distributions by life stage and over time

There were some differences in the estimated unstandardised distributions of Antipodean albatross, depending on the life stage and over time (Figures 3 to 5). The overall distribution showed areas of high use around the main colony of Antipodes Island, between the colony and the eastern end of Chatham rise, around Chatham rise (but not above it), and in two distinct areas along the west coast of South America (Figure 3). There was also relatively high use of Tasman Sea by individuals, but to a lesser extent.

Comparing the foraging areas between males and females showed distinct differences between east and west and north and south directions of the foraging range (Figure 4). Females tended to be more prevalent in the western area of the foraging range, and males tended to have a greater southern extent in their distribution.

When distributions were disaggregated by demographic group, there were state-specific trends in spatial use (Figure 5). Female breeders had a relatively restricted distribution centred on Antipodes Island, but female non-breeders foraged across the Pacific Ocean, including in areas on the west coast of South America. Similarly, male breeders also foraged close to Antipodes Island, whereas the distribution of male non-breeders extended eastward including the west coast of South America. Males also tended to utilise the area south of Chatham rise more than females, and tended to forage further south in the South Pacific Ocean area.

Juveniles used waters eastward of North Island New Zealand, especially north of Chatham rise, and the Tasman Sea extensively, but travelled smaller distances than adults.

Distribution time series (grouped by observation year) captured the key spatial trends evident in the aggregated map versions, but with particularly high inter-annual variability in years with low sample sizes (Appendix A, Figures A-1 and A-2).

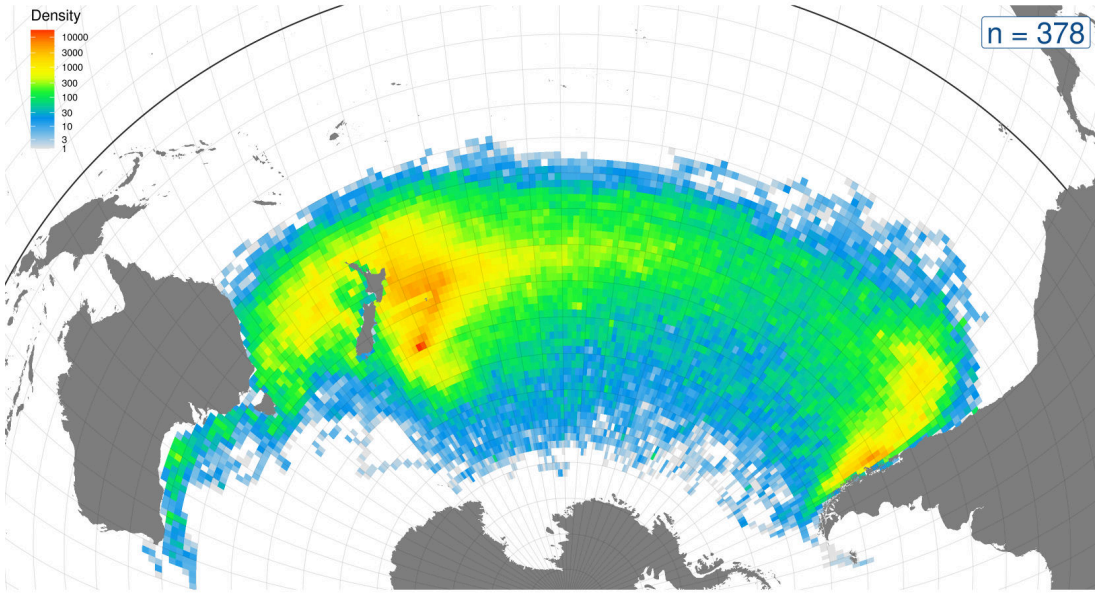

Figure 3: Density (in log-scale) of interpolated tag records for all years and tracked Antipodean albatross individuals combined, at 1-degree resolution. The number of tracks is shown in the top-right corner.

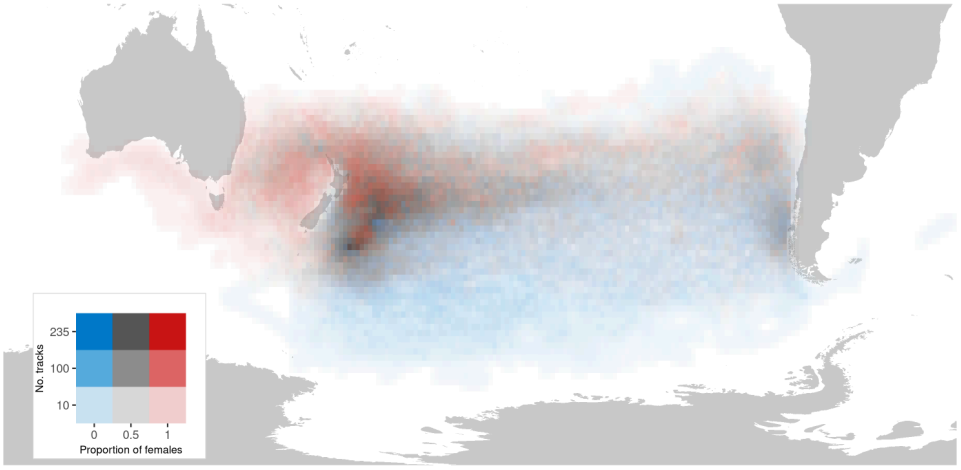

Figure 4: Sex ratio within the interpolated tag records for all years and tracked Antipodean albatross individuals combined, at 1-degree resolution.

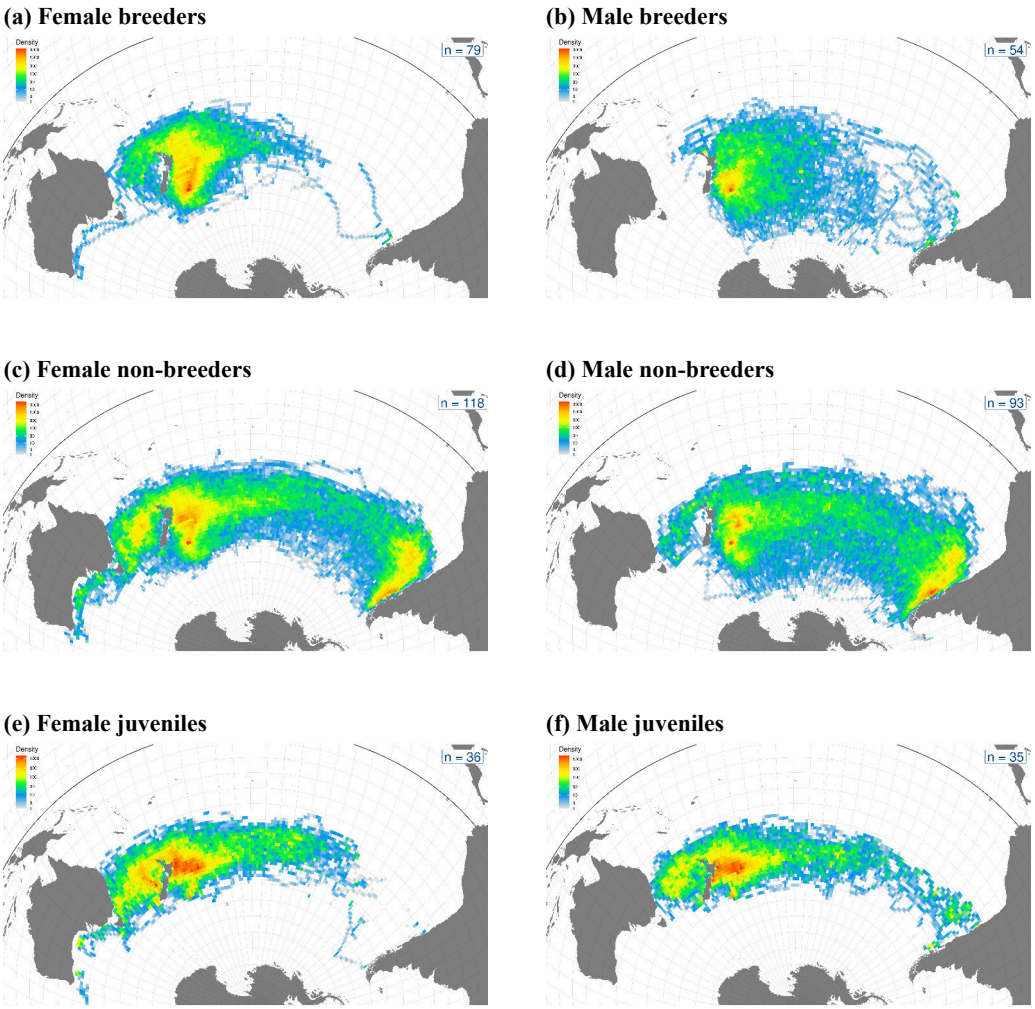

Figure 5: Density (in log-scale) of interpolated tag records for Antipodean albatross by demographic group for all years combined, at 1-degree resolution. The number of tracks for each demographic group is shown in the top-right corner.

3.3 Post-2011 changes in the distribution of non-breeders

A hybrid resampling-randomisation approach was developed to test for changes in distribution between two time periods while accounting for sample size and track length changes. The approach was applied to female and male non-breeders in separate analyses (Figures 6 and 7).

When track length was not standardised between time periods for female non-breeders, there was evidence (Pr(same) = 0.028) that there was a change in distribution between the pre-2004 and the post-2011 period (Figure 6). Nevertheless, once track length was standardised across time periods, the difference in the overlap metric measured between observed and randomised samples was not significant (Pr(same) = 0.142).

The overlap between pre-2004 and post-2011 distributions was higher for non-breeding males than for non-breeding females (Figure 7). There was no support for a difference between pre-2004 and post-2011 time periods (Pr(same) = 0.400) for non-breeding males. Accounting for track length across time periods reduced further the probability of difference between time periods (Pr(same) = 0.624).

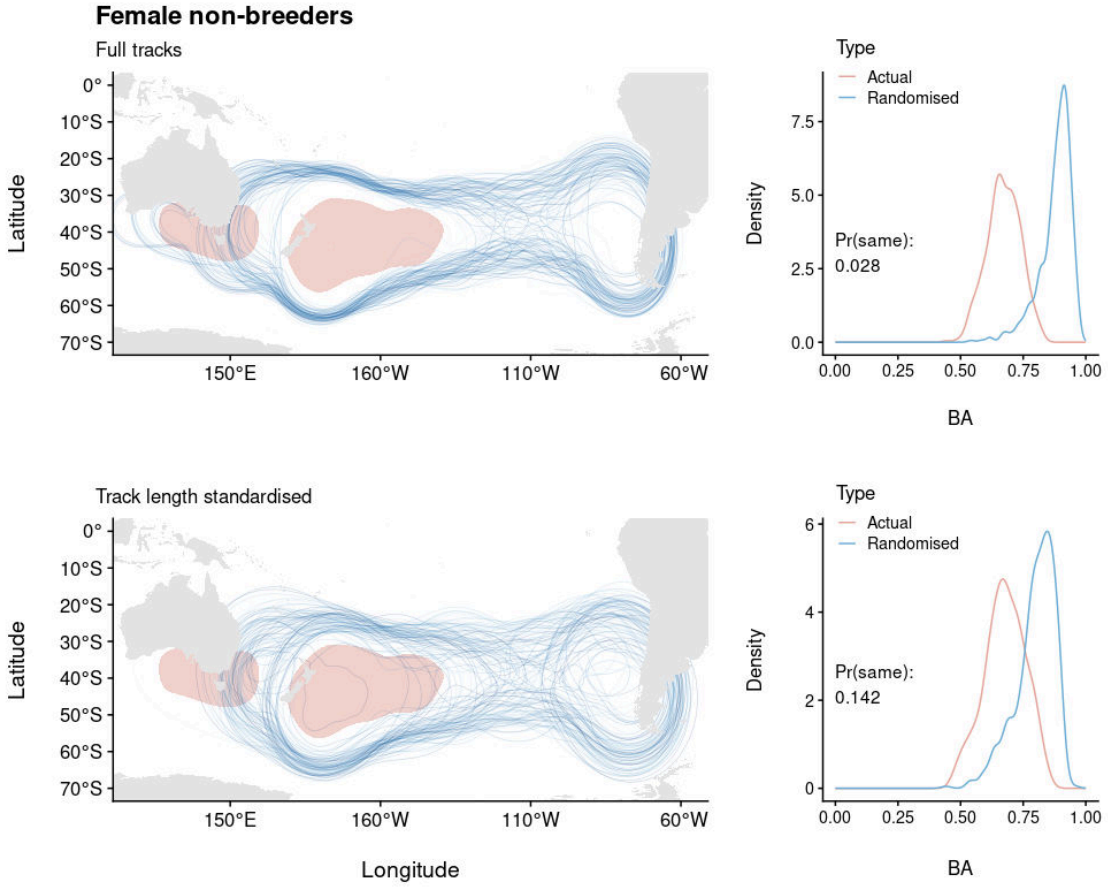

Figure 6: Summary of analyses testing differences in distribution for non-breeder females of Antipodean albatross between the periods 1996–2004 (pre-2004) and 2011–2022 (post-2011). Each map panel compares the 95% kernel density for the pre-2004 period (in red) to a sample of 100 kernel densities generated by resampling tracks from the post-2011 dataset (in shades of blue). Right column compares the distribution of Bhattacharyya's affinity (BA) metric of overlap for kernels based on the actual period when the track was recorded versus periods randomly assigned to tracks. Top panel shows the results using full tracks from the post-2011 period, and bottom panel shows the results using post-2011 track length standardised to match pre-2004 track lengths.

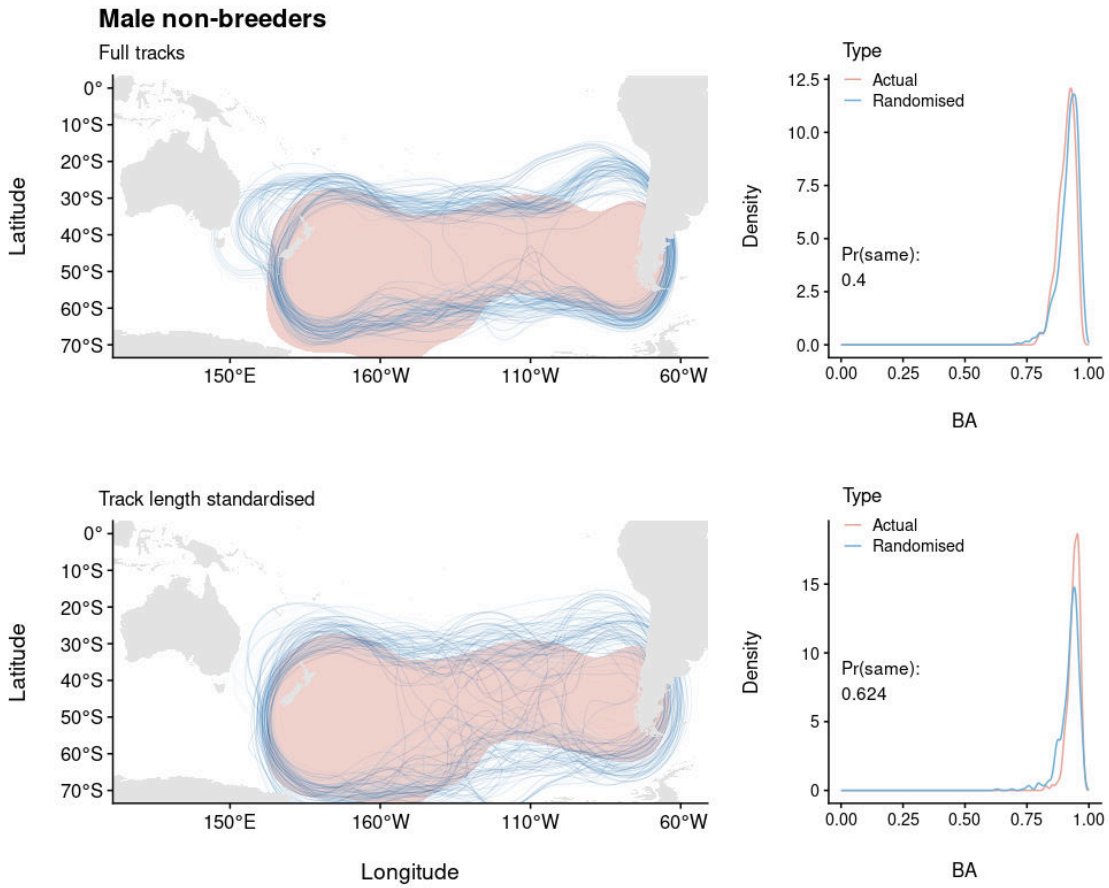

Figure 7: Summary of analyses testing differences in distribution for non-breeder males of Antipodean albatross between the periods 1996–2004 (pre-2004) and 2011–2022 (post-2011). Each map panel compares the 95% kernel density for the pre-2004 period (in red) to a sample of 100 kernel densities generated by resampling tracks from the post-2011 dataset (in shades of blue). Right-most column compares the distribution of Bhattacharyya's affinity (BA) metric of overlap for kernels based on the actual period when the track was recorded versus periods randomly assigned to tracks. Top panel shows the results using full tracks from the post-2011 period, and bottom panel shows the results using post-2011 track length standardised to match pre-2004 track lengths.

3.4 Distribution hotspots and hotspot variability through time

There were clear differences in the distribution of Antipodean albatross distribution hotspots between life stages (Figure 8). All life stages used the area immediately east of New Zealand intensively, with the highest use adjacent to the colony at Antipodes Island. Nevertheless, juveniles also used some areas in the Tasman Sea extensively, especially westward from New Zealand's Exclusive Economic Zone. Non-breeding adults had hotspots distributed across the South Pacific Ocean, including in the Tasman Sea and an extensive area off the Chilean coast at around latitude 44 °S and around the Juan Fernández Islands. Breeders had the most restricted hotspot area, concentrated around Antipodes Island, and extending northward to the tip of New Zealand.

When considering density hotspots for all life stages through time, there was some variability; earlier years with few tagged individuals showed the most variability compared with later years, when more data were available (Figure 9). There was some variability between years regarding a hotspot in the Tasman Sea, and also in the spatial extent of the hotspot area off the coast of Chile. When cells were classified as a function of the proportion of times, they were classified as a hotspot with a 99% confidence level; the two areas with the highest hotspot consistency were the areas eastward of New Zealand, including Antipodes Island, and the Chilean coast (Figure 10).

3.5 Final at-sea distribution maps

The final at-sea distributions of Antipodean albatross by population class and sex are shown in Figure 11.

3.6 Variability in the overlap with surface-longline fisheries

The combined at-sea distribution for all life stages of Antipodean albatross reflected the extensive range of this species in the Southern Hemisphere, from the west coast of Australia in the Indian Ocean to the Chilean coast in the east Pacific Ocean (Figure 12). The north end of the distribution was approximately bounded by the 25 °S parallel. The effort from surface-longline fisheries (administered through RFMOs) for years 1997 to 2019 was higher on the western side of the South Pacific Ocean and also north of the 20 °S parallel, but effort was distributed throughout the South Pacific Ocean (Figure 13).

Overall overlap varied between years and amongst fleets, with a peak in 2003 and a plateau from 2007 onwards (Figure 14). The two fleets with the highest overlap were the New Zealand and the Japanese surface-longline fleets. The areas with the highest consistency in overlap hotspots throughout the time period were the Tasman Sea (skewed towards the Australian east coast), an area including waters east and north of New Zealand's North Island, and the Chilean coast (Figure 15).

The spatial overlap between surface-longline fisheries administered through RFMOs and Antipodean albatross by year for the period from 1997 to 2019 is included in Appendix B (Figure B-1).

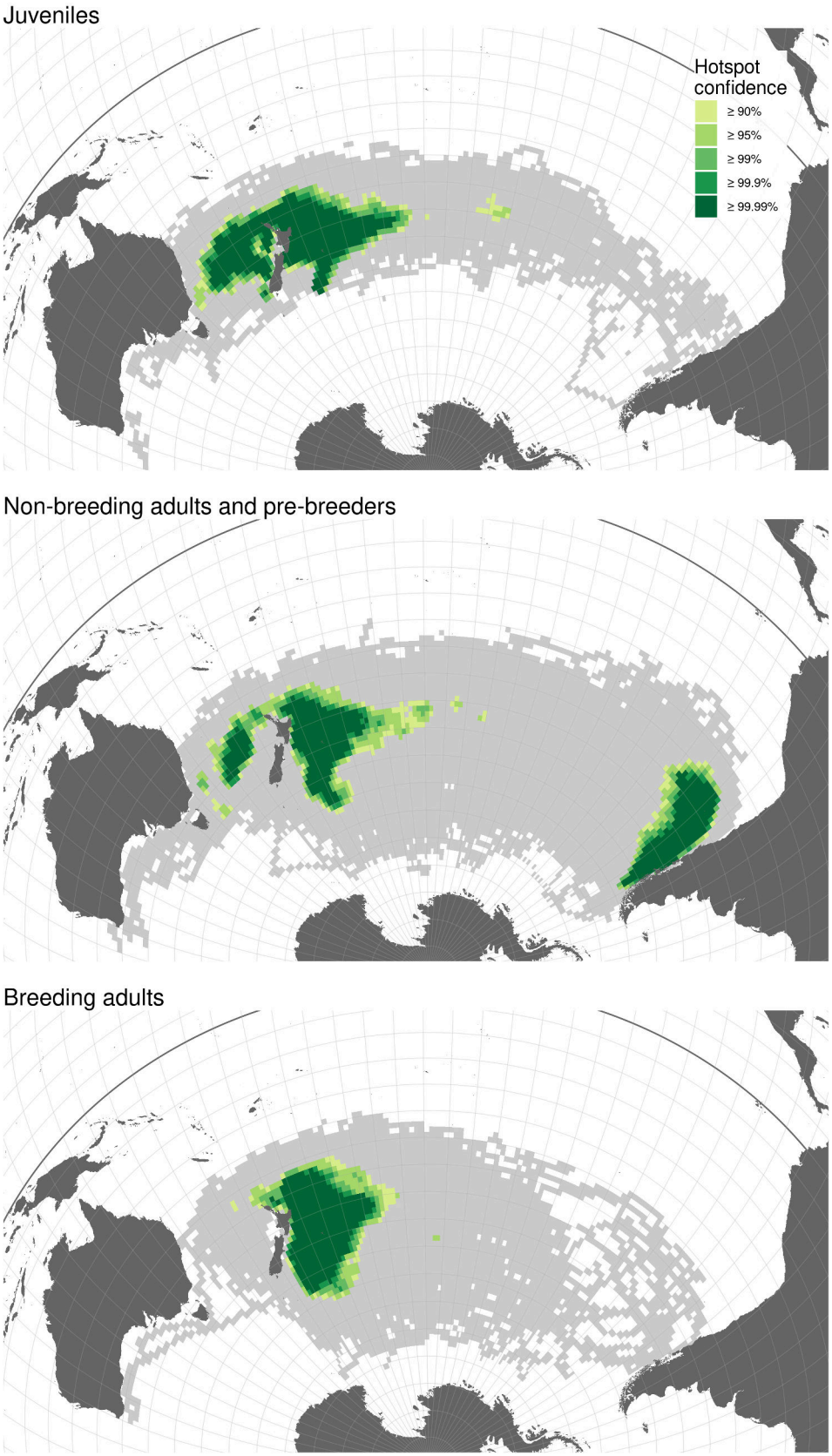

Figure 8: Distribution of Antipodean albatross hotspots for key life stages. Grey shading shows cells with at least one record, cells consisting of a hotspot are shown in shades of green as a function of the confidence level.

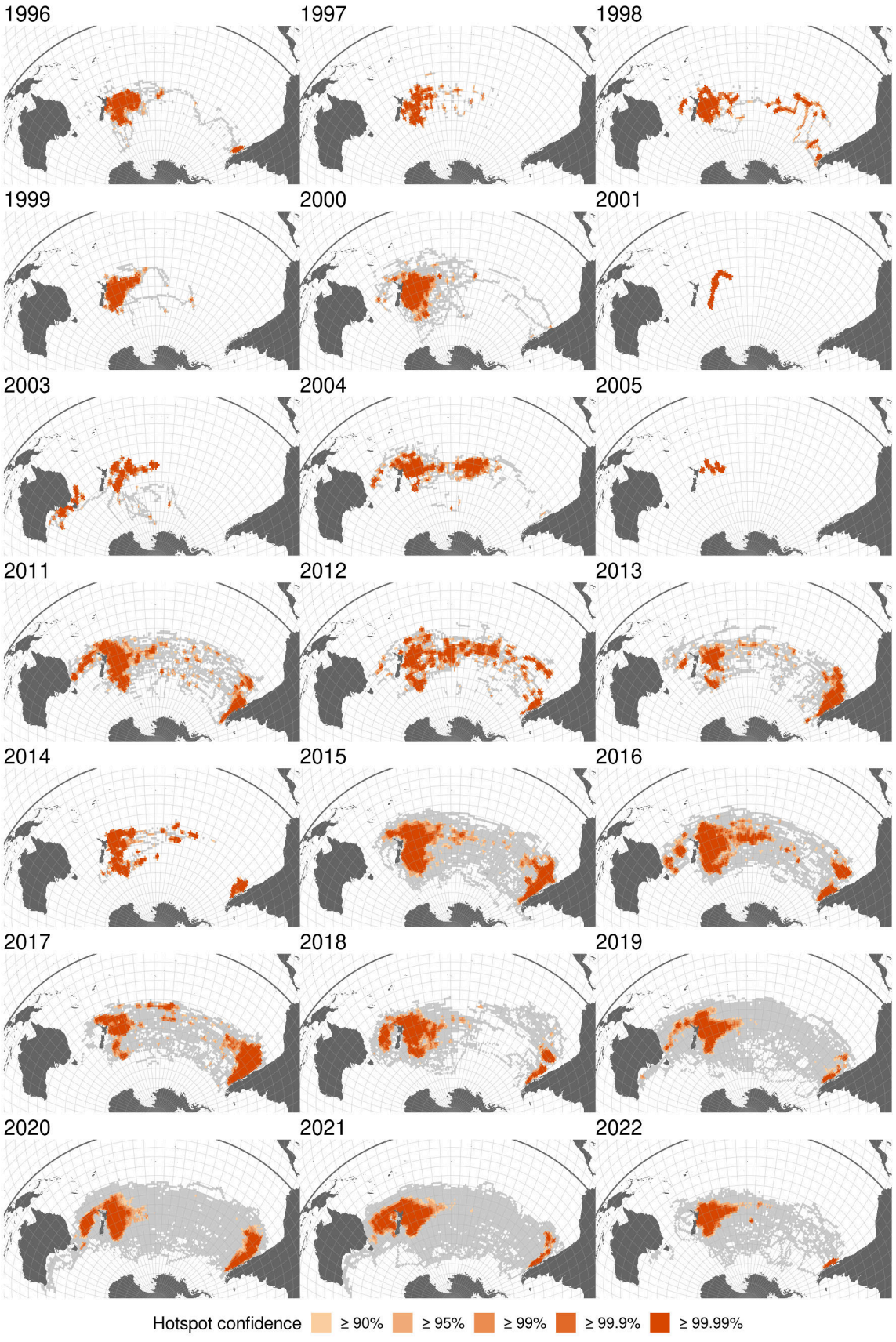

Figure 9: Distribution of Antipodean albatross hotspots for all years with tagging data, aggregated for all life stages. Grey shading shows cells with at least one record, cells consisting of a hotspot are shown in shades of red as a function of the confidence level.

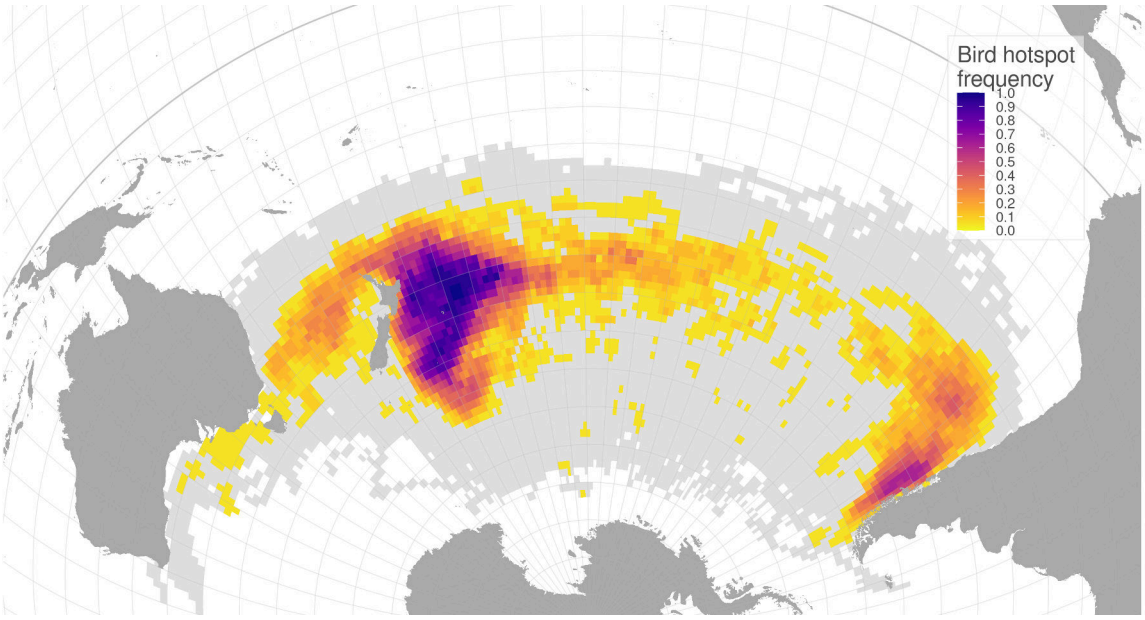

Figure 10: Temporal stability of Antipodean albatross distribution hotspots. The colour shows the proportion of years when a cell was identified as a hotspot of bird density, at a 99% confidence level. The light grey envelope represents the total extent of the distribution.

(a) Juvenile females

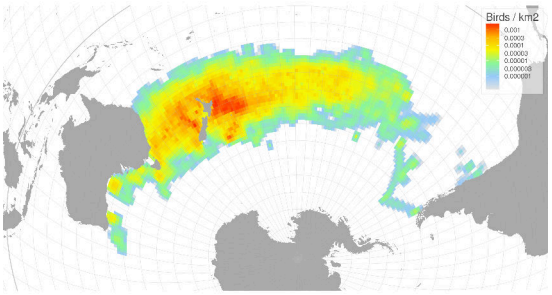

(b) Juvenile males

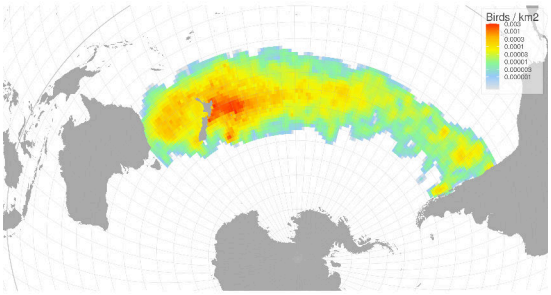

(c) Pre-breeding and non-breeding females

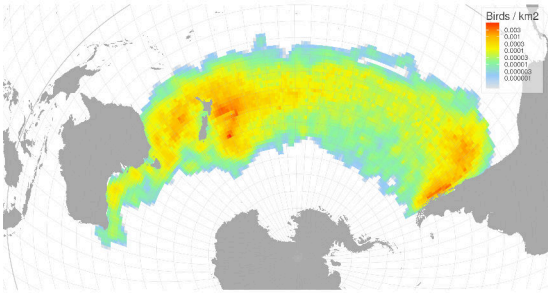

(d) Pre-breeding and non-breeding males

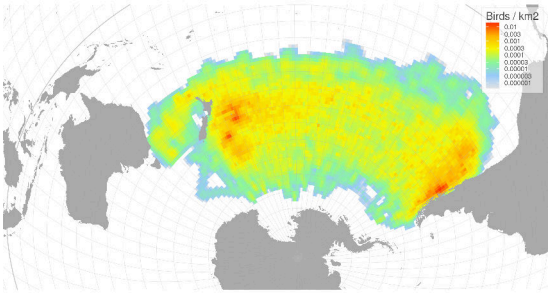

(e) Successfully breeding females

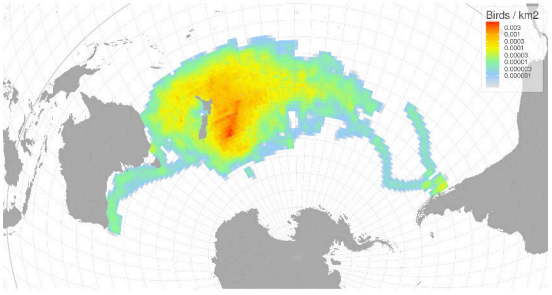

(f) Successfully breeding males

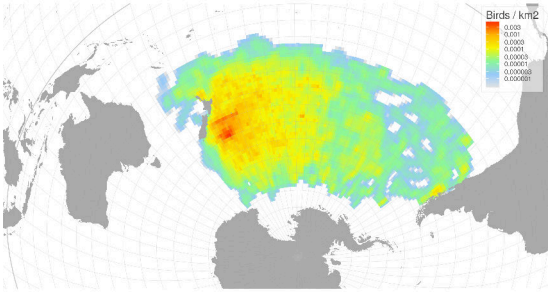

(g) Unsuccessfully breeding females

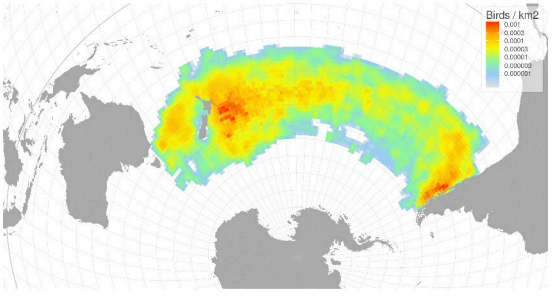

(h) Unsuccessfully breeding males

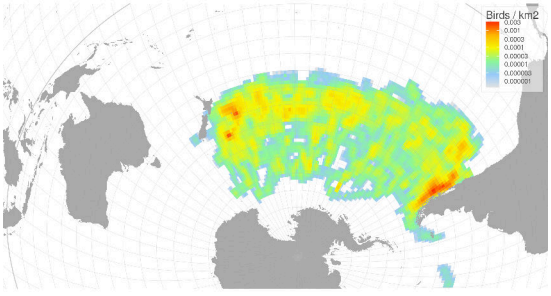

Figure 11: At-sea distribution of Antipodean albatross by population class and sex. The density of birds per square-kilometre is shown on a logarithmic scale.

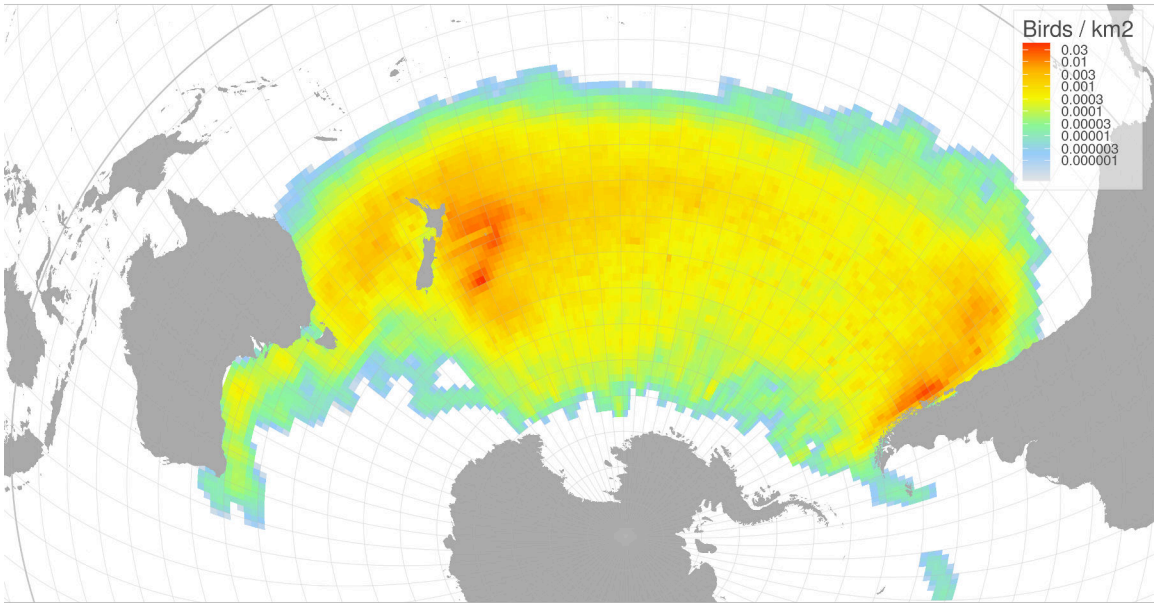

Figure 12: At-sea distribution of Antipodean albatross, after combining the distribution of each demographic stratum across all years between 1996 and 2022, weighted by the number of birds in each stratum obtained from an integrated population model. The colour is shown on a logarithmic scale.

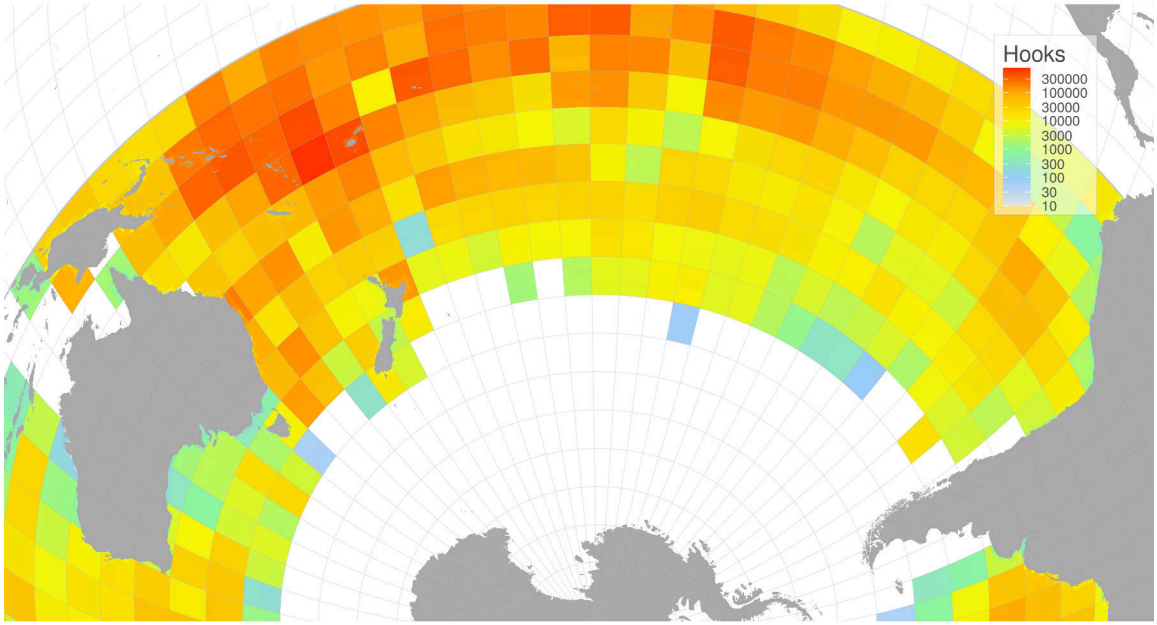

Figure 13: Mean annual surface-longline fishing effort (in number of hooks) between 1997 and 2019, coloured on a logarithmic scale.

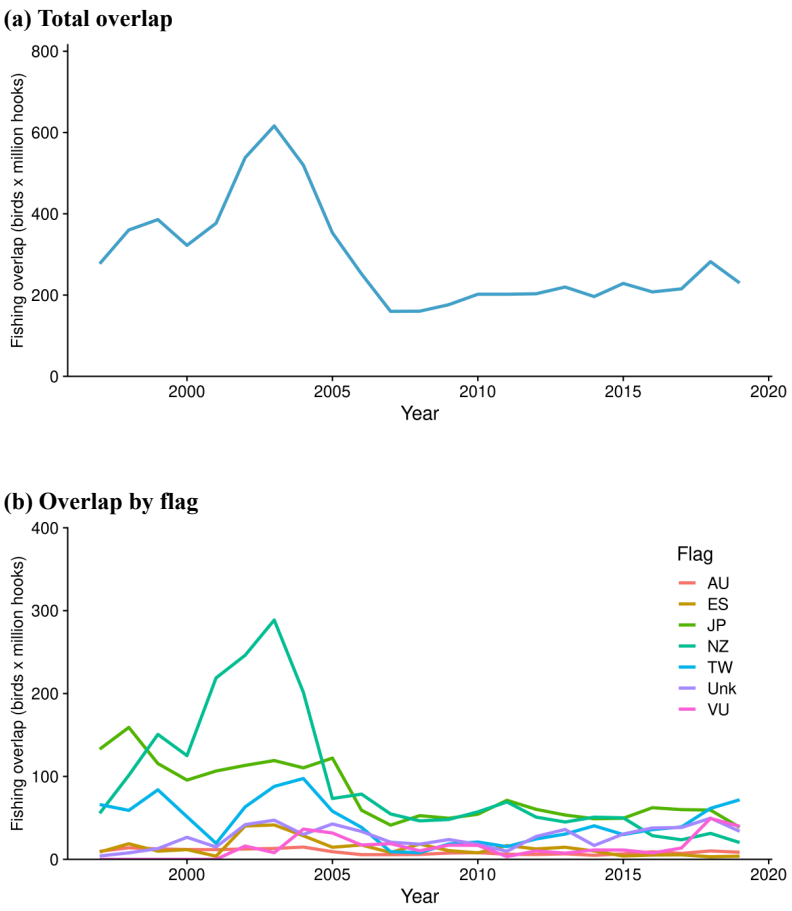

Figure 14: Interannual variability of the overlap between Antipodean albatross and surface-longline fishing effort, (a) across all fisheries, and (b) by vessel flag for all flags responsible for 99% of the total overlap (AU, Australia; ES, Spain; JP, Japan; NZ, New Zealand; TW, Taiwan; VU, Vanuatu; Unk, unknown).

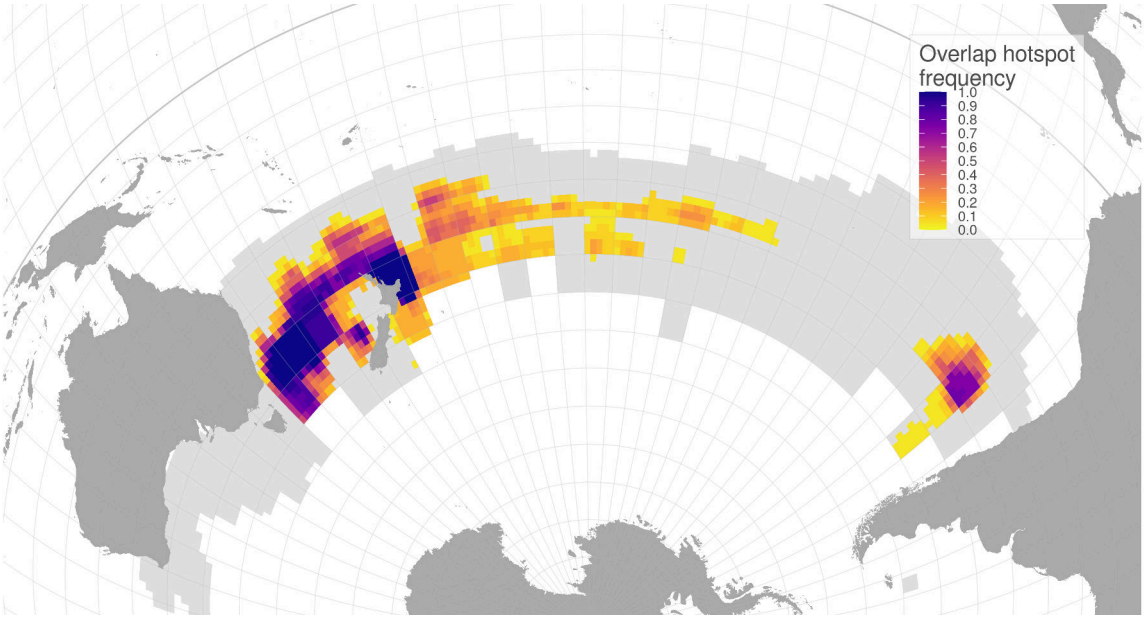

Figure 15: Temporal stability of overlap hotspots between Antipodean albatross and surface-longline fishing effort. The colour shows the proportion of years when each cell was identified as a hotspot of overlap, at a 99% confidence level. The light grey envelope represents the total extent of overlap.

4. DISCUSSION

This analysis highlighted key spatial differences in the distribution of Antipodean albatross by breeding status, age, and sex; it also further delineated the distribution of juvenile birds given increased tagging data for this group in the 2020 and 2021 breeding seasons. An improved distribution map was produced with all life stages combined, integrating all available tracking data with weights by life stage from a recent population model (Richard 2021). The distribution map was compared with surface-longline fishing effort in the Southern Hemisphere to assess variability in overlap hotspots. Although there was variability in the location of overlap hotspots through time, there were distinct areas that were consistently classified as hotspots in the time period from 1997 to 2019. These areas included the Tasman Sea, an area eastward and northward of New Zealand's North Island, and the Chilean coast.

Spatial overlap between Antipodean albatross and the surface-longline fleet was found to be highest for the New Zealand and Japanese fleets. This finding differs from the results of Bose & Debski (2021) who found highest overlap for the fleets of Chinese Taipei and Vanuatu (TW and VU), and little overlap with the New Zealand fleet for the year 2020 (although overlap varied across cohorts and years). Nevertheless, there were some key differences in methodology between the earlier analysis by Bose & Debski (2021) and the current assessment; most notably the effort dataset for the previous analysis was collated from Global Fishing Watch, and the effort variable was measured in hours. For the year 2019 only, the current analysis found the Chinese Taipei fleet to have the highest overlap followed by the Japanese fleet, which confirmed the importance of the Chinese Taipei fleet when quantifying interactions. Nevertheless, any estimates of overlap (and resulting captures) could vary depending on the effort dataset used to inform the analyses.

In addition, the earlier analysis by Bose & Debski (2021) derived stationary overlap from tracking data, compared with the present study, which used tracking data to derive predicted distributions of Antipodean albatross. This marked difference in approach may also account for differences in the findings between the two studies.

The hypothesis that the range of non-breeding females changed after 2010 was tested using a resampling approach developed to take into account the length of tracks which varied between periods due to the different tag types deployed over time. The analysis here provided some support that their distribution extended further east after 2010, but the difference was not statistically significant at a 0.05 level. This lack of statistical significance was most likely due to the small number of tracks prior to 2010, which limited the statistical power of the test.

The small number of tracks also prevented the production of two distinct distributions for the two periods. Instead, a single distribution was generated for both periods to retain maximum information.

The characterisation of density hotspots for key life stages highlighted two high-use zones beyond the area expected around the breeding colony: the Tasman Sea was especially important to juveniles (and to non-breeding adults to a lesser degree), whereas the Chilean east coast was especially important to non-breeding adults. These spatial patterns were not apparent for all years, which could reflect the different availability of tracks by life stages through time, and other factors such as long-term oceanography cycles like El Niño. When considered across the time series, however, these areas were consistently shown as hotspots, increasing confidence in the reliability of their classification. The approach of assessing hotspot areas and their consistency through time using the G_i* statistic is broadly applicable to other seabird species with tracking data.

The hotspot consistency approach was expanded to also assess overlap hotspots between Antipodean albatross and surface-longline fisheries; it succeeded in identifying areas with high overlap through time. One challenge in this application was the low resolution of the surface-longline effort dataset, which obscured some spatial patterns in the species' distribution. By increasing the resolution of the effort dataset, a higher-resolution delineation of overlap hotspots was obtained, but this approach relied on the assumption that effort was evenly distributed across 5-degree cells. Effort data recorded at a

higher resolution would improve precision in the identification of overlap hotspots. Also, the temporal variability in overlap was determined solely by changes in fishing effort, as a stationary distribution of Antipodean albatross was used due to the uneven coverage of the tracking dataset across demographic strata for most years. Additional data on fishing effort for 2020 and 2021, combined with the existing 2019 fishing effort data, could inform a comparison with annual bird distributions for the period 2019 to 2021 (which had higher coverage across demographic strata).

The considerable amount of tracking data collected for Antipodean albatross provided an in-depth understanding of their spatial ecology, differing among sexes, ages, and breeding status. It also revealed distinct areas of preferential foraging, consistent over time.

5. ACKNOWLEDGEMENTS

We thank Samhita Bose at the Department of Conservation for help with the tracking data.

We are also grateful to the Antipodean albatross working group for having allocated significant resources towards the collection of tracking data for the species.

The Aquatic Environment Working Group (hosted by Fisheries New Zealand) provided valuable feedback on an earlier version of this analysis. This project was funded under Fisheries New Zealand project PRO2021-06.

6. REFERENCES

Abraham, E.; Richard, Y.; Walker, N.; Gibson, W.; Daisuke, O.; Tsuji, S.; Kerwarth, S.; Winkler, H.; Parsa, M.; Small, C.; Waugh, S. (2019). *Assessment of the risk of surface longline fisheries in the Southern Hemisphere to albatrosses and petrels, for 2016*. Prepared for the 13th meeting of the Ecologically Related Species Working Group (ERSWG13) of the Commission for the Conservation of Southern Bluefin Tuna (CCSBT). https://www.ccsbt.org/en/system/files/ERSWG13_17_NZ_Assessment_RiskOfSurfaceLonglineFisheries_SouthernHemisphere.pdf

Abraham, E.; Richard, Y.; Walker, N.; Roux, M.-J. (2017). Assessment of the risk of commercial surface longline fisheries in the Southern Hemisphere to ACAP seabird species. Paper prepared for the 12th meeting of the Ecologically Related Species Working Group (ERSWG12).

Bose, S.; Debski, I. (2021). Antipodean albatross spatial distribution and fisheries overlap 2020. Prepared by the Department of Conservation. 36 p.

Calado, J.G.; Ramos, J.A.; Almeida, A.; Oliveira, N.; Paiva, V.H. (2021). Seabird-fishery interactions and bycatch at multiple gears in the Atlantic Iberian coast. *Ocean & Coastal Management 200*: 105306.

Calenge, C. (2006). The package "adehabitat" for the R software: A tool for the analysis of space and habitat use by animals. *Ecological modelling 197 (3–4)*: 516–519.

Carneiro, A.P.; Pearmain, E.J.; Oppel, S.; Clay, T.A.; Phillips, R.A.; Bonnet-Lebrun, A.-S.; Wanless, R.M.; Abraham, E.; Richard, Y.; Rice, J.; et al. (2020). A framework for mapping the distribution of seabirds by integrating tracking, demography and phenology. *Journal of Applied Ecology 57*: 514–525.

Elliott, G.; Walker, K. (2017). Antipodean wandering albatross census and population study 2017 [Report prepared by Albatross Research. 20 p]. https://www.doc.govt.nz/globalassets/documents/conservation/marine-and-coastal/marine-conservation-services/reports/antipodean-albatross-adams-island-2017.pdf

Fieberg, J.; Kochanny, C.O. (2005). Quantifying home-range overlap: The importance of the utilization distribution. *The Journal of Wildlife Management 69 (4)*: 1346–1359.

Francis, M.P.; Hoyle, S.D. (2019). Estimation of fishing effort in the Southern Hemisphere [28 p]. *New Zealand Aquatic Environment and Biodiversity Report No. 213*. https://fs.fish.govt.nz/Doc/24693/AEBR-2019-213-Fishing-effort-Southern-hemisphere%20(1).pdf.ashx

Getis, A.; Ord, J.K. (2010). The analysis of spatial association by use of distance statistics. *In*: Anselin, L. and Rey S.J. (eds.) Perspectives on spatial data analysis (pp. 127–145). Springer.

Grémillet, D.; Ponchon, A.; Paleczny, M.; Palomares, M.-L.D.; Karpouzi, V.; Pauly, D. (2018). Persisting worldwide seabird-fishery competition despite seabird community decline. *Current Biology 28 (24)*: 4009–4013.

Merkel, B.; Phillips, R.A.; Descamps, S.; Yoccoz, N.G.; Moe, B.; Strøm, H. (2016). A probabilistic algorithm to process geolocation data. *Movement ecology 4 (1)*: 1–11.

Pettex, E.; David, L.; Authier, M.; Blanck, A.; Dorémus, G.; Falchetto, H.; Laran, S.; Monestiezl, P.; Canneyt, O.V.; Virgili, A.; et al. (2017a). Using large scale surveys to investigate seasonal variations in seabird distribution and abundance. Part I: The North Western Mediterranean Sea. *Deep Sea Research Part II: Topical Studies in Oceanography 141*: 74–85.

Pettex, E.; Laran, S.; Authier, M.; Blanck, A.; Dorémus, G.; Falchetto, H.; Lambert, C.; Monestiez, P.; Stéfan, E.; Canneyt, O.V.; et al. (2017b). Using large scale surveys to investigate seasonal variations in seabird distribution and abundance. Part II: The Bay of Biscay and the English Channel. *Deep Sea Research Part II: Topical Studies in Oceanography 141*: 86–101.

Ramos, R.; Carlile, N.; Madeiros, J.; Ramírez, I.; Paiva, V.H.; Dinis, H.A.; Zino, F.; Biscoito, M.; Leal, G.R.; Bugoni, L.; et al. (2017). It is the time for oceanic seabirds: Tracking year-round distribution of gadfly petrels across the Atlantic Ocean. *Diversity and Distributions 23 (7)*: 794–805.

Rayner, M.J.; Taylor, G.A.; Gummer, H.D.; Phillips, R.A.; Sagar, P.M.; Shaffer, S.A.; Thompson, D.R. (2012). The breeding cycle, year-round distribution and activity patterns of the endangered Chatham petrel (*Pterodroma axillaris*). *Emu-Austral Ornithology 112 (2)*: 107–116.

Richard, Y. (2021). *Integrated population model of Antipodean albatross for simulating management scenarios*. BCBC2020-09 final report prepared by Dragonfly Data Science for the Conservation Services Programme, Department of Conservation, Wellington. 31 p. https://www.doc.govt.nz/globalassets/documents/conservation/marine-and-coastal/marine-conservation-services/reports/final-reports/bcbc2020-09-antipodean-albatross-simulations-final-report2.pdf

Sussman, A.L.; Gardner, B.; Adams, E.M.; Salas, L.; Kenow, K.P.; Luukkonen, D.R.; Monfils, M.J.; Mueller, W.P.; Williams, K.A.; Leduc-Lapierre, M.; et al. (2019). A comparative analysis of common methods to identify waterbird hotspots. *Methods in Ecology and Evolution 10 (9)*: 1454–1468.

Waugh, S.; Troup, C.; Filippi, D.; Weimerskirch, H. (2002). Foraging zones of southern royal albatrosses. *The Condor 104 (3)*: 662–667.

APPENDIX A: Times series of distributions by observation year

(a) Female breeders

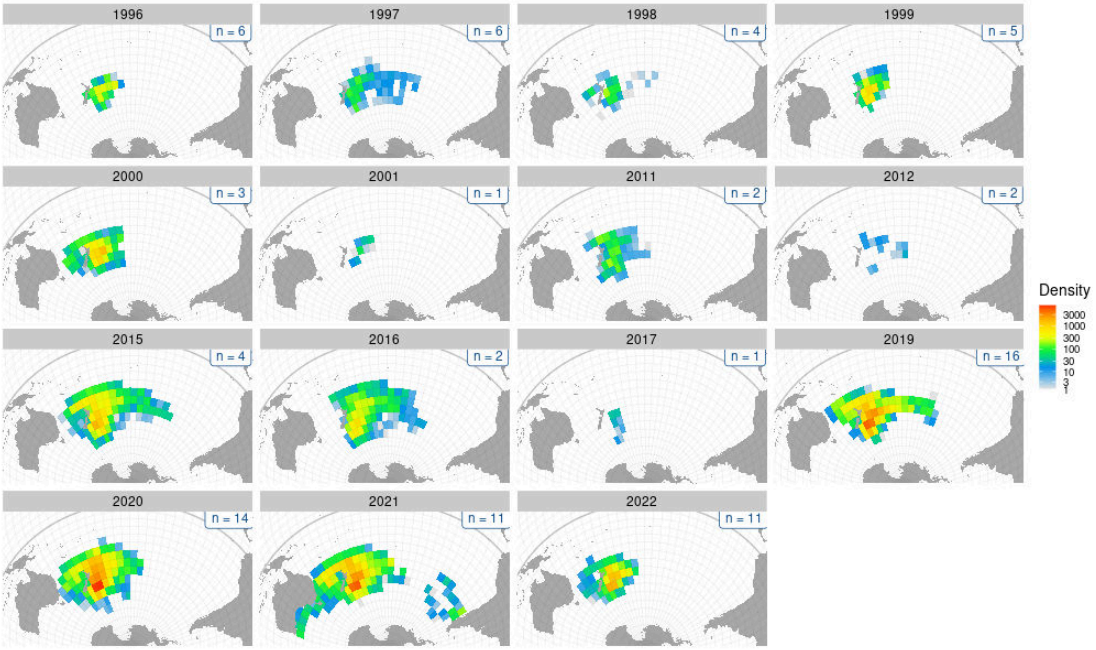

(b) Female non-breeders

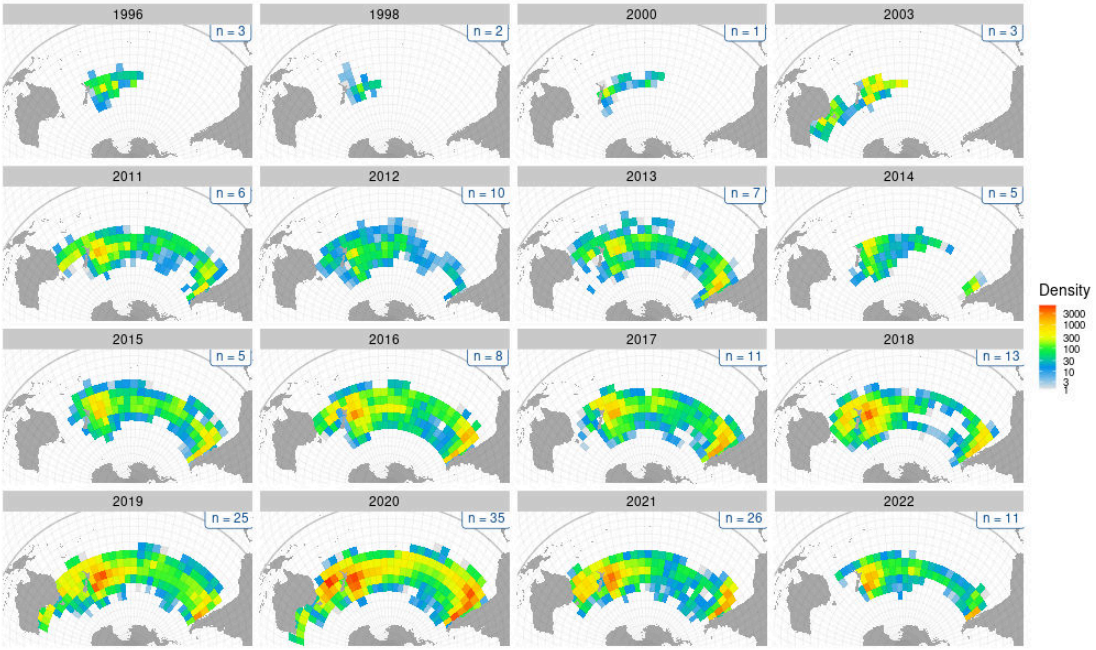

Figure A-1: Density (in log-scale) of interpolated tag records for female Antipodean albatross by observation year, for both breeders (a) and non-breeders (b), at 5-degree resolution. The number of tracks by year is shown in the top-right corner of each panel.

(a) Male breeders

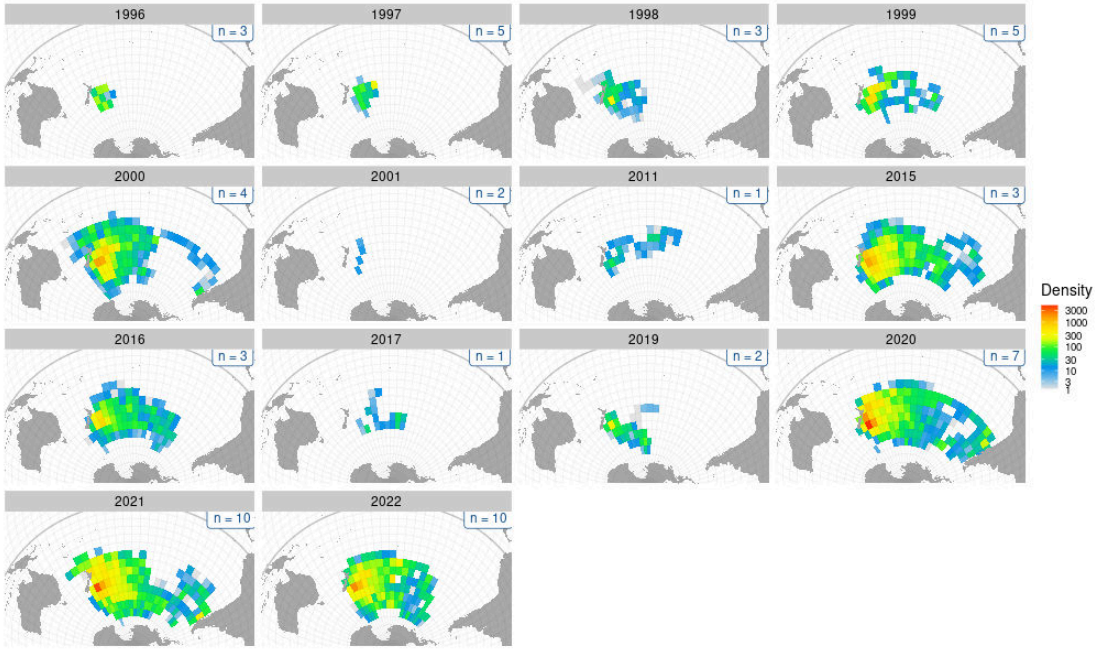

(b) Male non-breeders

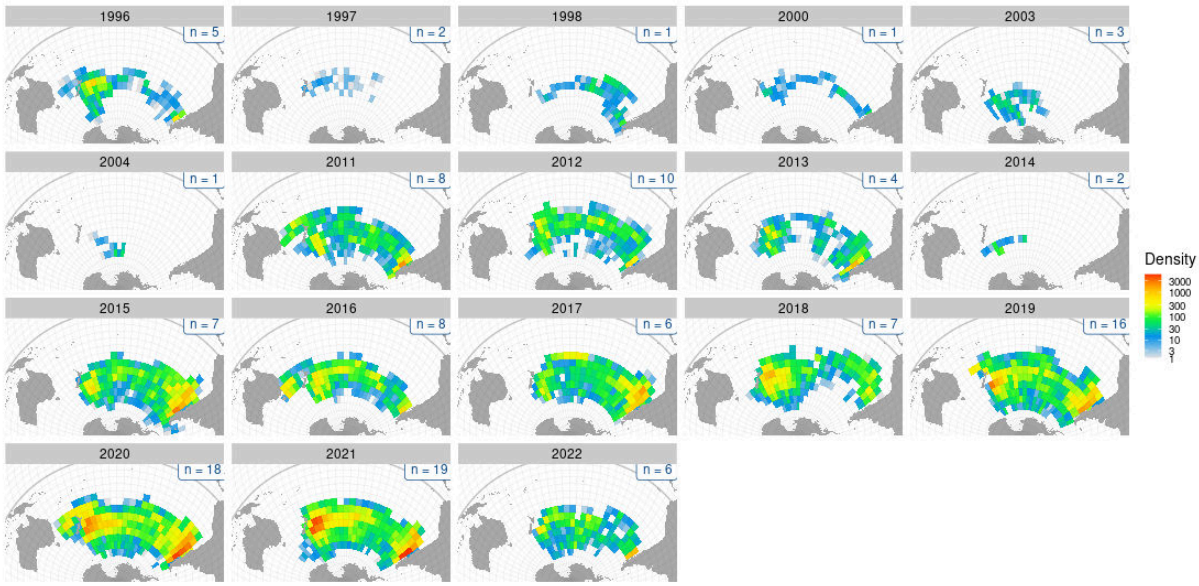

Figure A-2: Density (in log-scale) of interpolated tag records for male Antipodean albatross by observation year, for both breeders (a) and non-breeders (b), at 5-degree resolution. The number of tracks by year is shown in the top-right corner of each panel.

APPENDIX B: Overlap with surface-longline fisheries by year

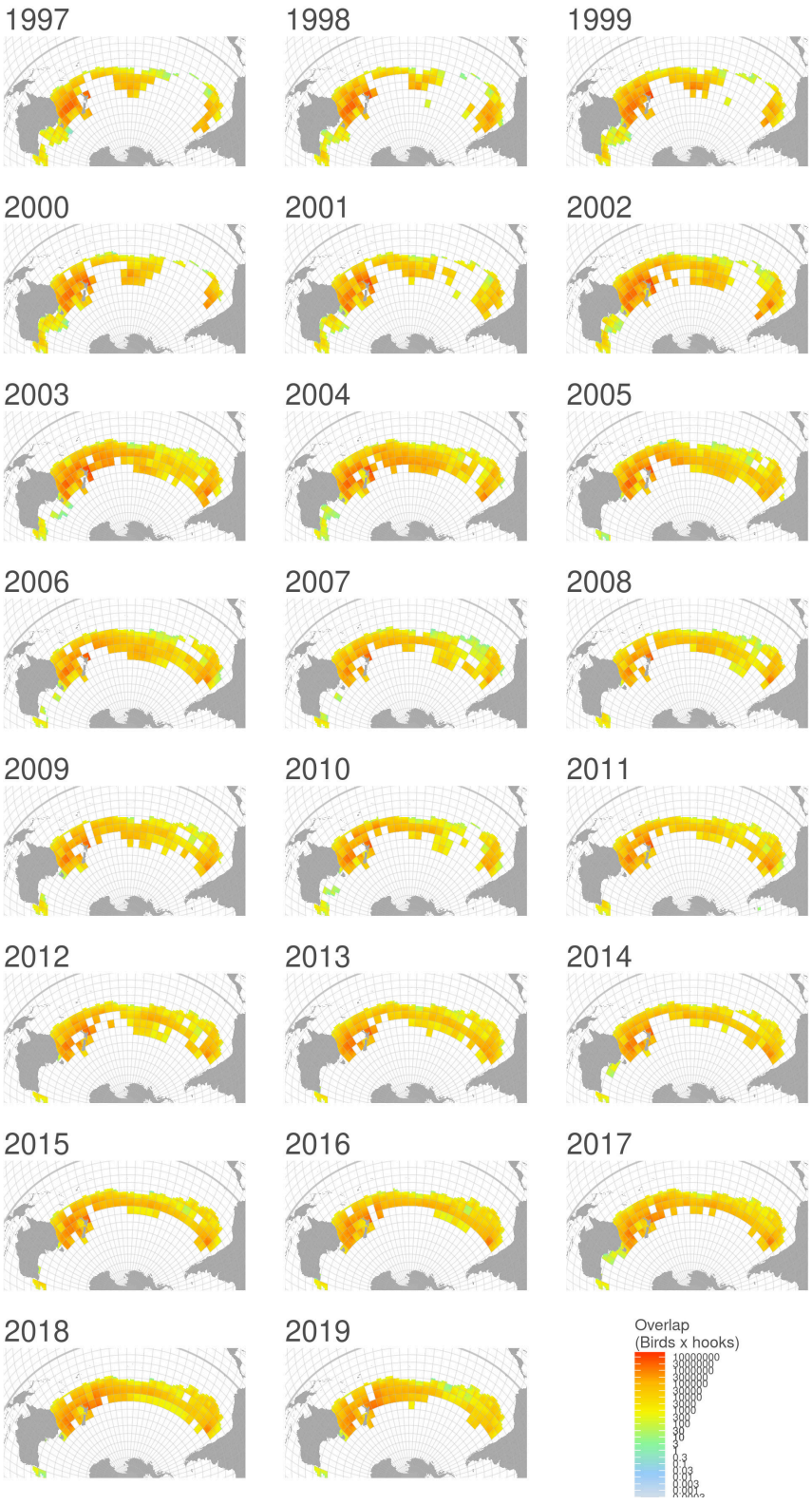

Figure B-1: Spatial overlap in the distribution of Antipodean albatross and surface-longline fishing effort in the Southern Hemisphere by year for the period 1997 to 2019.